Georgia Southern University

Digital Commons@Georgia Southern

10-1-2008

Erasing Dark Matter Cusps in Cosmological Galactic Halos with Baryons

Emilio Romano-Diaz

Isaac Shlosman

Yehuda Hoffman

Clayton Heller

Ⓔ

ERASING DARK MATTER CUSPS IN COSMOLOGICAL GALACTIC HALOS WITH BARYONS

EMILIO ROMANO-DÍAZ,[1] ISAAC SHLOSMAN,[1] YEHUDA HOFFMAN,[2] AND CLAYTON HELLER[3]

ABSTRACT

We study the central dark matter (DM) cusp evolution in cosmologically grown galactic halos. Numerical models with and without baryons (baryons+DM, hereafter BDM model, and pure DM, PDM model, respectively) are advanced from identical initial conditions, obtained using the Constrained Realization method. The DM cusp properties are contrasted by a direct comparison of pure DM and baryonic models. We find a divergent evolution between the PDM and BDM models within the inner few $\times$ 10 kpc region. The PDM model forms an R^{-1} cusp as expected, while the DM in the BDM model forms a larger isothermal cusp R^{-2} instead. The isothermal cusp is stable until $z \sim 1$ when it gradually levels off. This leveling proceeds from inside out and the final density slope is shallower than -1 within the central 3 kpc (i.e., expected size of the R^{-1} cusp), tending to a flat core within $\sim$2 kpc. This effect cannot be explained by a finite resolution of our code which produces only a 5% difference between the gravitationally softened force and the exact Newtonian force of point masses at 1 kpc from the center. Neither is it related to the energy feedback from stellar evolution or angular momentum transfer from the bar. Instead it can be associated with the action of DM+baryon subhalos heating up the cusp region via dynamical friction and forcing the DM in the cusp to flow out and to "cool" down. The process described here is not limited to low z and can be efficient at intermediate and even high z.

Subject headings: dark matter — galaxies: evolution — galaxies: formation — galaxies: halos — galaxies: interactions — galaxies: kinematics and dynamics

Online material: color figures

1. INTRODUCTION

Cosmological numerical simulations of pure dark matter (DM) halo formation have led to "universal" density profile which can be approximated by $\rho(r) = 4\rho_s/(r/R_s)(1 + r/R_s)^2$ (Navarro et al. 1997, NFW), with R_s being a characteristic "inner" radius where logarithmic density slope is -2 and ρ_s is the density at R_s. This profile steepens outside R_s and tends to a cusp $\sim R^{-1}$ toward the center, at $R_{\rm cusp} \sim 0.1R_s$. While this profile remains invariant under mergers (El-Zant 2008), its origin is yet to be explained (e.g., Syer & White 1998; Nusser & Sheth 1999; Shapiro et al. 2005; Ascasibar et al. 2007).

The NFW density profile is a source of an ongoing controversy—its universality in the numerical pure DM models is in apparent contradiction with at least some of the observations of disk galaxies and galaxy clusters, which exhibit rather flat density cores (e.g., Flores & Primack 1994; Kravtsov et al. 1998; Salucci & Burkert 2000; Sand et al. 2002; de Blok et al. 2003; de Blok 2005, 2007; Simon et al. 2003; but see Rhee et al. 2004; answered by Gentile et al. 2004, 2005; Kuzio de Naray et al. 2008). While a number of "exotic" explanations involving less conventional physics have been proposed, attempts to resolve this discrepancy within the CDM cosmology have been made as well. The DM cusp leveling off was attributed to the DM-baryon interactions, such as a dynamical friction of DM/baryon inhomogeneities (i.e., substructure) against the DM halo background (El-Zant et al. 2001, 2004; Tonini et al. 2006), stellar bar–DM interaction (Weinberg & Katz 2002; Holley-Bockelmann et al. 2005; but see Sellwood 2003; McMillan & Dehnen 2005; Dubinski et al. 2008), and baryon energy feedback (e.g., Mashchenko et al. 2006; Peirani et al. 2008). In this Letter, we test the first option

(El-Zant et al.)—the effect of the baryon+DM substructure in the fully self-consistent numerical simulations of halo formation in the ΛCDM cosmology with WMAP3 parameters (more details in Romano-Díaz et al. 2008).

Early arguments about change of the central density profile claimed that baryons drag DM in the so-called adiabatic contraction, steepening the DM density slope (e.g., Blumenthal et al. 1986). However, they have neglected the clumpy nature of the accreting material in the assembling halo, which can give rise to clump-background dynamical friction and energy transfer from the clumps to the background. The ability of baryons to radiate their internal energy increases the binding energy and acts as a "glue" on the DM substructure (El-Zant et al. 2001). El-Zant et al. have used the Monte Carlo technique to calculate the leveling of the NFW cusp in the presence of such clumps and found this process to be efficient over $\sim$1–2 Gyr. The initial conditions presumed the existence of an NFW cusp, a spherically symmetric DM halo and indestructible clumps.

The NFW cusp is characterized by the "temperature" (i.e., DM dispersion velocities) inversion which makes it thermodynamically improbable but dynamically stable in the absence of an energy transfer mechanism (El-Zant et al. 2001). Dynamical friction of sufficiently bound clumps can trigger such energy flux into the cusp, increasing its dispersion velocities and washing it out. El-Zant et al. found that the necessary condition for the dynamical friction to have an effect is the aggregation of mass into the clumps more massive than $\sim 10^{-4}$ of the DM halo—a result confirmed for the galaxy clusters as well (El-Zant et al. 2004).

In fully self-consistent numerical simulations with baryons, the question is whether the NFW cusp forms in the first place. Such simulations have been either limited to high redshifts ($z = 3.3$; Gnedin et al. 2004) or focused on the adiabatic contraction and had an insufficient resolution (Gustafsson et al. 2006). They have verified that baryons lead to a steeper DM

[1] Department of Physics and Astronomy, University of Kentucky, Lexington, KY 40506-0055.
[2] Racah Institute of Physics, Hebrew University, Jerusalem 91904, Israel.
[3] Department of Physics, Georgia Southern University, Statesboro, GA 30460.
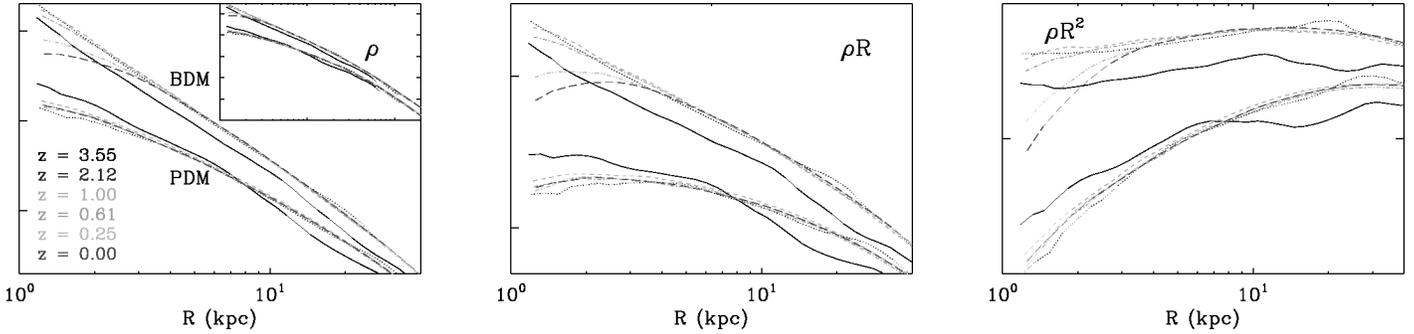
FIG. 1.—Redshift evolution of DM density profiles $\rho(R)$ (*left*), $\rho(R)R$ (*middle*), and $\rho(R)R^2$ (*right*) in PDM and BDM models: $z = 3.55$ (*solid curve*), 2.12 (*dotted curve*), 1.0 (*dashed curve*), 0.61 (*dot-dashed curve*), 0.25 (*double-dot-dashed curve*), and 0 (*long-dashed curve*). The PDM and BDM curves are displaced vertically for clarity. The inner 40 kpc of halos are shown. The vertical coordinate units are logarithmic and arbitrary. For the PDM model, the density is well fitted by the NFW profile over a large range in z, and $R_s \sim 28$ kpc at $z = 0$. For the BDM model, the NFW fit is worse and $R_{\rm iso} \sim 15$ kpc at the end. The inset provides ρ within a 200 kpc range for a comparison. [*See the electronic edition of the Journal for a color version of this figure.*]

density profile than the NFW cusp, but left open its subsequent evolution. This issue is addressed here.

2. NUMERICS AND INITIAL CONDITIONS

Numerical simulations have been performed with the FTM 4.5 hybrid N-body/SPH code (Heller & Shlosman 1994; Heller et al. 2007; Romano-Díaz et al. 2008) using physical and not comoving coordinates. The number of DM particles is 2.2×10^6 and the SPH particles—4×10^5. The gravity is computed with the falcON routine (Dehnen 2002) which scales as O(N). The gravitational softening (P1 of falcON) is $\epsilon_{\rm grav} = 500$ pc, for DM, stars, and gas. The calculated force differs by ~5% from the exact Newtonian force between point masses at $R \sim 2\epsilon_{\rm grav} = 1$ kpc. We assume the ΛCDM cosmology with WMAP3 parameters, $\Omega_m = 0.24$, $\Omega_\Lambda = 0.76$, and $h = 0.73$, where h is the Hubble constant in units of 100 km s^{-1} Mpc^{-1}. The variance $\sigma_8 = 0.76$ of the density field convolved with the top-hat window of radius 8 h^{-1} Mpc^{-1} was used to normalize the power spectrum. The star formation algorithm is described in Heller et al. (2007). Several generations of stars are allowed to form from an SPH particle. The energy and momentum feedback into the ISM is implemented, and the relevant parameters are (Heller et al.): the energy thermalization $\epsilon_{\rm SF} = 0.3$, the cloud gravitational collapse $\alpha_{\rm ff} = 1$, and the self-gravity fudge factor $\alpha_{\rm crit} = 0.5$.

The initial conditions generated here are those of Romano-Díaz et al. (2008): we use the Constrained Realizations (CR) method (Hoffman & Ribak 1991) within a restricted volume of 8^3 h^{-1} Mpc, where a 5 h^{-1} Mpc sphere is carved out and evolved. The constructed Gaussian field is required to obey a set of constraints of arbitrary amplitudes and positions (e.g., Romano-Díaz et al. 2006, 2007). Two constraints were imposed on the initial density field: first, that the linear field Gaussian smoothed with a kernel of 1.0×10^{12} h^{-1} $M_\odot$ has an overdensity of $\delta = 3$ at the origin (2.5 σ perturbation, where σ^2 is the variance of the appropriately smoothed field). It was imposed on a 256^3 grid and predicted to collapse by $z_c \sim 1.33$ by the top-hat model. This perturbation is embedded in a region (second constraint) corresponding to 5×10^{13} h^{-1} $M_\odot$ in which the overdensity is zero, i.e., the unperturbed universe. The random component of the CR introduces density perturbations on all scales, thus leading to major mergers (Romano-Díaz et al. 2006, 2007). The mass inside the computational sphere is ~6.1 $\times$ 10^{12} h^{-1} $M_\odot$. In the baryonic model, we have randomly

replaced 1/6 of DM particles by equal-mass SPH particles. Hence, Ω_m is not affected.

3. DM DENSITY AND VELOCITY DISPERSION PROFILES

Two models analyzed here are those of a pure DM (hereafter PDM) and DM+baryons (BDM). Evolution of DM density profiles for both models is shown in Figure 1 at various redshifts and in three different ways: as $\rho(R)$ per se, factored by R, and by R^2, in order to emphasize the R^{-1} and R^{-2} cusps. At early redshifts, $z \sim 7$, the DM density profiles of both models are nearly identical. With time, the BDM halo becomes more cuspy—the DM experiencing the adiabatic contraction by baryons. This region of higher density extends gradually to larger R, up to ~15 kpc at $z = 0$. Between $z \sim 4$ and 1 the DM density profile becomes and remains nearly isothermal within this region—$\rho(R)R^2$ is flat there (Fig. 1, *right panel*). In comparison, the PDM halo exhibits the slope of -2 at $R_s \sim 28$ kpc only, as expected, with the NFW cusp size $R_{\rm cusp} \sim 3$ kpc at $z = 0$. Hence over prolonged time period, while the PDM model displays the NFW cusp, the DM in the BDM model remarkably forms an isothermal cusp, down to the central kpc, i.e., to $\sim 2\epsilon_{\rm grav}$. The isothermal cusp in the BDM model is gradually erased inside $R_{\rm iso} \sim 15$ kpc after $z \sim 1$. In fact, within the central 3 kpc it becomes flatter than -1, i.e., flatter than the NFW cusp, as seen in all three panels of Figure 1, and within ~ 2 kpc forms a rather flat core. At $z = 0$, the PDM model is denser outside $R_{\rm iso}$, while BDM remains denser within this radius.

Furthermore, in the PDM model, the density around 1 kpc from the center stays virtually unchanged after $z \sim 3$. The baryonic model shows a somewhat different behavior. Namely, it keeps the same DM density at 1 kpc between $z \sim 3$ and 0.7, which decays thereafter by a factor of ~3.

Behavior of the velocity dispersions, $\sigma_{\rm DM}$, in both models mirrors that of the density. The NFW DM cusp in the PDM model forms early and is characterized by the "temperature" inversion as shown in Figure 2, where we display the z evolution of the DM dispersion velocities (see also El-Zant et al. 2001). In contrast, the BDM model shows a cuspy distribution of $\sigma_{\rm DM}(R)$, which after $z \sim 4$ can be approximated well by a single power law, $\sigma_{\rm DM}(R)^2 \sim R^{-\beta}$, inside the central 10 kpc. The evolution of $|\beta|$ is shown in Figure 3 for both models. It is steadily increasing in the PDM model until the end of the major mergers epoch at $z \sim 1.5$, where it levels off. The BDM model shows a similar increase in $|\beta|$, but well beyond the mergers epoch, until $z \sim 0.7$, where
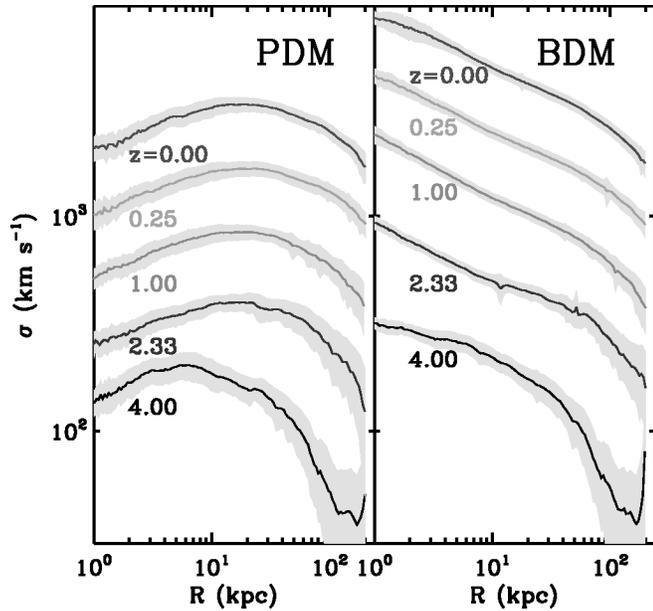
FIG. 2.—Redshift evolution of DM velocity dispersions in PDM (*left*) and BDM (*right*) models. Except for the lowest ones, the curves are displaced vertically up for clarity. The second curves (from the bottom) are displaced by a factor of 2, the third by a factor of 2^2, the fourth by a factor of 2^3, and the last ones by a factor of 2^4. The colored width represents a 1 σ dispersion around the mean. The inner 200 kpc of halos are shown. The vertical coordinate units are logarithmic. [*See the electronic edition of the Journal for a color version of this figure.*]

it sharply declines. This decline in β is crucial in understanding the fate of the density cusp, as we discuss below.

4. DISCUSSION

We have performed a direct comparison between the DM halo evolution in the pure DM and baryonic models, from identical cosmological initial conditions. Our goal is to understand the effect of the baryons on the DM density profile. We, therefore, focus on the DM evolution within the central region, quantify the cuspiness of the density distribution there, and attempt to relate its evolution to that of the DM substructure. Our results show that the DM in the PDM model has established an NFW cusp early, and the only subsequent changes we observe are related to sudden increases in R_s at the time of the major mergers (e.g., Romano-Díaz et al. 2006, 2007). On the other hand, the baryonic (BDM) model goes through a two-step process: first, in the central ~10 kpc, the DM is dragged in by the baryons in what fits the adiabatic contraction (e.g., Gnedin et al. 2004; Gustafsson et al. 2006). This stage is concurrent with the formation and growth of a galactic disk, but we did not verify whether the disk is solely responsible for the DM contraction. For an extended period of time, after $z \sim 4$, an isothermal cusp forms with $\rho_{DM} \sim R^{-2}$ and persists. In the next step, the DM cusp is being gradually washed out from inside out, mainly after $z \sim 1$. By $z = 0$, the isothermal cusp is largely erased, and the density slope within the central 10 kpc is less steep than -2. In fact within the central ~3 kpc, it is less steep than the NFW slope of -1. We note that the *DM in the BDM model does not form the NFW cusp in the first place, but rather by-passes it in favor of an isothermal DM cusp which is subsequently washed out*. For example, the "temperature" inversion characteristic of the NFW cusp is never observed in the BDM model (Fig. 2).

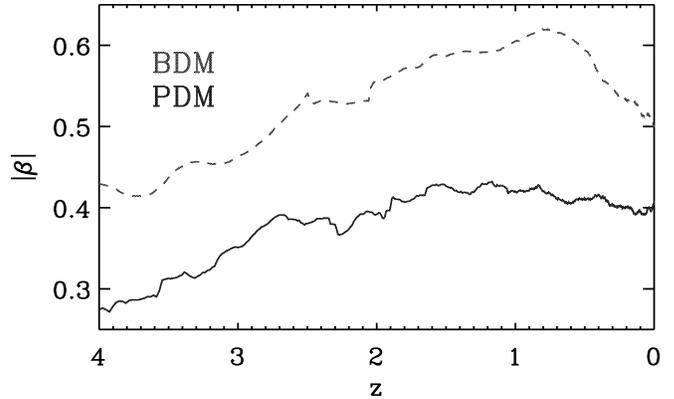We first argue that this leveling of the DM cusp is not a

FIG. 3.—Redshift evolution of the power index $|\beta|$ in the PDM (*solid curve*) and BDM (*dashed curve*) models. Here β is calculated by fitting a power law $\sigma_{DM}^2 \sim R^{-\beta}$ between 1 and 10 kpc. Note that $\beta > 0$ for BDM and $\beta < 0$ for PDM models. [*See the electronic edition of the Journal for a color version of this figure.*]

numerical artifact, i.e., is not caused by a finite resolution of the code which is $2\epsilon_{grav} = 1$ kpc. At this distance, softened and exact Newtonian forces between point masses differ by 5%—this cannot account for the observed changes in density profile farther out. We also note that the DM density peak in the BDM model is occasionally offset from the baryonic peak by a few kpc, around $z \sim 1$ and especially at 0.4, with the subhalos influx into the center, in what can be treated as $m = 1$ instability. Therefore, we have fitted the DM halo profile based on the position of the DM density peak at each frame. The cusp will be "smeared" if this procedure is not followed (McMillan & Dehnen 2005). Also, the prime halo moves with respect to the center of mass of the computational sphere; this is related to the residual large-scale streaming motions in the DM (Romano-Díaz et al. 2008).

Next, we note that most of the cusp leveling happens after $z \sim 1$ (Fig. 1). This correlates with a decrease in the slope of the central dispersion velocities (Fig. 2). The slope change in β (Fig. 3) comes from the decrease in the central dispersion velocities around few kpc, while σ_{DM} at $R \sim 10$ kpc remains unchanged. What is the reason for this apparent "cooling" of the isothermal DM cusp?

Any decrease in central σ_{DM} of a dissipationless self-gravitating entity in virial equilibrium is counterintuitive. It clearly has nothing to do with the major mergers, as this epoch ends at $z \sim 1.5$ in our models. Any subsequent *smooth* accretion of dissipative baryons will only increase σ_{DM} as a result of the ongoing adiabatic contraction. However, if one considers accretion of *clumpy* baryons, which act as a "glue" on the DM subhalos where they reside, an additional process of "heating" the DM by means of a dynamical friction becomes important. The heating rate is skewed to the density peak and will cause the DM to stream out of the cusp's gravitational well, eventually decreasing the "temperature" gradient at the center. Figure 3 displays this behavior of β after it reaches its peak at $z \sim 0.7$. For a comparison, the PDM halo shows a flat β after the epoch of major mergers, for nearly 10 Gyr.

Central region crossing by subhalos (as well as accretion and tidal disruption) continues to the present time. Why do changes in the cusp become significant after $z \sim 1$? Figure 4 displays the evolution of the subhalo population within the central 30 kpc of the BDM halo. We observe that at least in two instances, $z \sim 1$ and 0.4, there is a clear excess in the BDM subhalo population, corresponding to the splash in the subhalo influx rates. The number of these subhalos also exceeds that
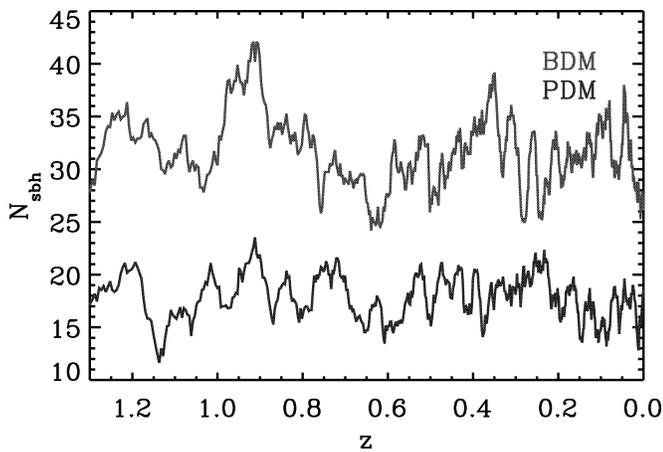
FIG. 4.—Evolution of the subhalo number N_{sbh} within central 30 kpc of the prime halo with redshift—PDM (*lower curve*) and BDM (*upper curve*). Note the sharp increase in N_{sbh} for the BDM model after $z \sim 1$, 0.5, and 0.2. [*See the electronic edition of the Journal for a color version of this figure.*]

of the PDM by ~ 2. The BDM subhalos appear in waves within the central region and these waves coincide with the DM streaming out of the center and "cooling" down. Hence, the process of washing out the DM cusp correlates with the influx of subhalos into the innermost region of the BDM halo. We show elsewhere that waves of subhalos crossing the central region of the prime halo originate in the filament, cluster there, and enter the prime halo before they merge among themselves.

We find that the mass distribution of subhalos (in the computational sphere) with masses M_{sbh} evolves with redshift—at high $z \gtrsim 4$ it can be approximated by a power law, $N_{sbh} \sim M_{sbh}^{-1}$, both in PDM and BDM models (Romano-Diaz et al. 2008). But in the central virialized 100 kpc of the halo it evolves differently from the field subhalos. Specifically, it is heavily skewed toward more massive ones after $z \sim 1$, while that of the PDM subhalos is only weakly so. This is significant, because the efficiency of dynamical friction increases substantially with the clump-to-prime halo virial mass ratio (El-Zant

et al. 2001). At $z \sim 4$, this ratio for the most massive subhalo residing within the virialized halo is ~ 0.06. By $z \sim 1$ this ratio is $\sim 10^{-3}$, and at $z = 0$ it is $\sim 8 \times 10^{-4}$—still higher than the minimum required by El-Zant et al.

The size of the obtained core in the DM distribution of the BDM model can be compared with observationally inferred cores. Following Salucci et al. (2007), for the virial mass of our halo at $z = 0, M_{vir} \sim 4 \times 10^{12} M_{\odot}$, the expected core is ~ 1.6 kpc. Spano et al. (2008) lists a large range of core sizes, starting from ~ 1 kpc. Both are compatible with the value obtained here.

In summary, we find that the DM density cusp corresponding to R_{cusp} in the PDM model is leveled off by the action of subhalos in the presence of baryons in the BDM model. The energy feedback from stellar evolution has decayed by this time without any effect on the cusp. We do not detect the angular momentum (J) transfer from the bar to the cusp—the latter J stays constant in time. We also find that the BDM model forms a steeper isothermal rather than NFW-type cusp for extended time period. It goes through a two-step process which involves gravitational contraction, followed by the influx of subhalos which heat up and dissolve the cusp.

Our models, although containing about 1.6×10^6 particles per halo, are still insufficient to fully resolve the formation of substructure around the prime halo. They should be viewed rather as a lower limit on the efficiency of the process reported here. Neither is the process described here limited to low z— one can easily envision scenario(s) when the subhalos act at intermediate and even high z. Overall, this work stands in agreement with Gnedin et al. (2004) who stopped the simulation at redshift $z = 3.3$, well before the leveling of the density cusp. However, Gustafsson et al. (2006) barely lacked resolution to detect the cusp behavior observed here. We have recently learned that J. P. Ostriker (private communication) obtained similar results on the cusp flattening.

REFERENCES

Ascasibar, Y., Hoffman, Y., & Gottloeber, S. 2007, MNRAS, 376, 393
Blumenthal, G. R., Faber, S. M., Flores, R., & Primack, J. R. 1986, ApJ, 301, 27
de Blok, W. J. G. 2005, ApJ, 634, 227
de Blok, W. J. G. 2007, in Island Universes, ed. R. S. de Jong (Dordrecht: Springer), 89
de Blok, W. J. G., Bosma, A., & McGaugh, S. 2003, MNRAS, 340, 657
Dehnen, W. 2002, J. Comput. Phys., 179, 27
Dubinski, J., Berentzen, I., & Shlosman, I. 2008, ApJ, submitted
El-Zant, A. 2008, ApJ, 681, 1058
El-Zant, A., Shlosman, I., & Hoffman, Y. 2001, ApJ, 560, 636
El-Zant, A. A., Hoffman, Y., Primack, J., Combes, F., & Shlosman, I. 2004, ApJ, 607, L75
Flores, R. A., & Primack, J. R. 1994, ApJ, 427, L1
Gentile, G., Burkert, A., Salucci, P., Klein, U., & Walter, F. 2005, ApJ, 634, L145
Gentile, G., Salucci, P., Klein, U., Vergani, D., & Kalberla, P. 2004, MNRAS, 351, 903
Gnedin, O. Y., Kravtsov, A. V., Klypin, A. A., & Nagai, D. 2004, ApJ, 616, 16
Gustafsson, M., Fairbairn, M., & Sommer-Larsen, J. 2006, Phys. Rev. D, 74, 123522
Heller, C. H., & Shlosman, I. 1994, ApJ, 424, 84
Heller, C. H., Shlosman, I., & Athanassoula, E. 2007, ApJ, 671, 226
Hoffman, Y., & Ribak, E. 1991, ApJ, 380, L5
Holley-Bockelmann, K., Weinberg, M., & Katz, N. 2005, MNRAS, 363, 991
Kravtsov, A. V., Klypin, A. A., Bullock, J. S., & Primack, J. R. 1998, ApJ, 502, 48

Kuzio de Naray, R., McGaugh, S. S., & de Blok, W. J. G. 2008, ApJ, 676, 920
Mashchenko, S., Couchman, H. M. P., & Wadsley, J. 2006, Nature, 442, 539
McMillan, P. J., & Dehnen, W. 2005, MNRAS, 363, 1205
Navarro, J., Frenk, C., & White, S. D. M. 1997, ApJ, 490, 493 (NFW)
Nusser, A., & Sheth, R. K. 1999, MNRAS, 303, 685
Peirani, S., Kay, S., & Silk, J. 2008, A&A, 479, 123
Rhee, G., Valenzuela, O., Klypin, A., Holtzman, J., & Moorthy, B. 2004, ApJ, 617, 1059
Romano-Díaz, E., Hoffman, Y., Heller, C. H., Faltenbacher, A., Jones, D., & Shlosman, I. 2006, ApJ, 637, L93
———. 2007, ApJ, 657, 56
Romano-Díaz, E., Shlosman, I., Heller, C. H., & Hoffman, Y. 2008, ApJ, submitted
Salucci, P., & Burkert, A. 2000, ApJ, 537, L9
Salucci, P., Lapi, A., Tonini, C., Gentile, G., Yegorova, I., & Klein, U. 2007, MNRAS, 378, 41
Sand, D. J., Treu, T., & Ellis, R. S. 2002, ApJ, 574, L129
Sellwood, J. A. 2003, ApJ, 587, 638
Shapiro, P. R., et al. 2005, in Progress in Dark Matter Research, ed. J. V. Blain (New York: Nova Science Publishers), astro-ph/0409173
Simon, J. D., Bolatto, A. D., Leroy, A., & Blitz, L. 2003, ApJ, 596, 957
Spano, M., et al. 2008, MNRAS, 383, 297
Syer, D., & White, S. D. M. 1998, MNRAS, 293, 337
Tonini, C., Lapi, A., & Salucci, P. 2006, ApJ, 649, 591
Weinberg, M. D., & Katz, N. 2002, ApJ, 580, 627